REPORT

# Identification of *KLHL41* Mutations Implicates BTB-Kelch-Mediated Ubiquitination as an Alternate Pathway to Myofibrillar Disruption in Nemaline Myopathy

Vandana A. Gupta,[1] Gianina Ravenscroft,[2] Ranad Shaheen,[3] Emily J. Todd,[2] Lindsay C. Swanson,[1] Masaaki Shiina,[4] Kazuhiro Ogata,[4] Cynthia Hsu,[1] Nigel F. Clarke,[5] Basil T. Darras,[6] Michelle A. Farrar,[7] Amal Hashem,[3] Nicholas D. Manton,[8] Francesco Muntoni,[9] Kathryn N. North,[10] Sarah A. Sandaradura,[5] Ichizo Nishino,[11] Yukiko K. Hayashi,[11] Caroline A. Sewry,[9] Elizabeth M. Thompson,[12,13] Kyle S. Yau,[2] Catherine A. Brownstein,[1] Timothy W. Yu,[1] Richard J.N. Allcock,[14] Mark R. Davis,[15] Carina Wallgren-Pettersson,[16] Naomichi Matsumoto,[17] Fowzan S. Alkuraya,[3] Nigel G. Laing,[2] and Alan H. Beggs[1,*]

Nemaline myopathy (NM) is a rare congenital muscle disorder primarily affecting skeletal muscles that results in neonatal death in severe cases as a result of associated respiratory insufficiency. NM is thought to be a disease of sarcomeric thin filaments as six of eight known genes whose mutation can cause NM encode components of that structure, however, recent discoveries of mutations in non-thin filament genes has called this model in question. We performed whole-exome sequencing and have identified recessive small deletions and missense changes in the Kelch-like family member 41 gene (*KLHL41*) in four individuals from unrelated NM families. Sanger sequencing of 116 unrelated individuals with NM identified compound heterozygous changes in *KLHL41* in a fifth family. Mutations in *KLHL41* showed a clear phenotype-genotype correlation: Frameshift mutations resulted in severe phenotypes with neonatal death, whereas missense changes resulted in impaired motor function with survival into late childhood and/or early adulthood. Functional studies in zebrafish showed that loss of Klhl41 results in highly diminished motor function and myofibrillar disorganization, with nemaline body formation, the pathological hallmark of NM. These studies expand the genetic heterogeneity of NM and implicate a critical role of BTB-Kelch family members in maintenance of sarcomeric integrity in NM.

Nemaline myopathy (NM) is a rare congenital disorder primarily affecting skeletal muscle function. Clinically, NM is a heterogeneous group of myopathies of variable severity.[1,2] The "severe" congenital form of NM presents with reduced or absent spontaneous movements in utero leading to severe contractures or fractures at birth and respiratory insufficiency leading to early mortality. Individuals with the "intermediate" congenital form of NM have antigravity movement and independent respiration at delivery but exhibit delayed motor milestones and require ventilatory support later in life. The "typical" congenital form of NM usually presents in the neonatal period or first year of life with hypotonia, weakness, and feeding difficulties with less prominent respiratory involvement. In these cases, the disease is usually static or very slowly progressive, and many individuals remain ambulant for much of their lives.[3] The defining diagnostic feature of all forms of NM, irrespective of genetic mutation, is the presence of numerous red-staining rods with Gomori trichrome stain that appear as rod-shaped electron-dense structures termed "nemaline bodies" by electron microscopy.[4] These nemaline bodies are most frequently cytoplasmic; however, the presence of intranuclear rods has also been reported.[5]

NM is a genetically heterogeneous condition, and mutations in eight different genes have been identified that are associated with dominant and/or recessive forms of this disease.[6–13] Mutations in these genes cause about 75%–80% of NM cases, suggesting the involvement of additional unidentified genes in disease etiology.

[1]Division of Genetics and Genomics, The Manton Center for Orphan Disease Research, Boston Children's Hospital, Harvard Medical School, Boston, MA 02115, USA; [2]Western Australian Institute for Medical Research and the Centre for Medical Research, University of Western Australia, Nedlands, Western Australia 6009, Australia; [3]Developmental Genetics Unit, King Faisal Specialist Hospital and Research Center, Riyadh 11211, Saudi Arabia; [4]Department of Biochemistry, Yokohama City University, Graduate School of Medicine, 3-9 Fukuura, Kanazawa-ku, Yokohama 236-0004, Japan; [5]Institute for Neuroscience and Muscle Research, Children's Hospital at Westmead and Discipline of Paediatrics and Child Health, University of Sydney, Sydney 2145, Australia; [6]Department of Neurology, Boston Children's Hospital, Harvard Medical School, Boston, MA 02115, USA; [7]Department of Neurology, Sydney Children's Hospital, Randwick NSW 2032, Australia; [8]Department of Surgical Pathology, SA Pathology at the Women's and Children's Hospital, North Adelaide, South Australia 5006; [9]Dubowitz Neuromuscular Centre, Institute of Child Health and Great Ormond Street Hospital, London WC1N 1EH, UK; [10]Murdoch Childrens Research Institute, The Royal Children's Hospital, Parkville, Victoria 3052, Australia; [11]Department of Neuromuscular Research, National Institute of Neuroscience, National Center of Neurology and Psychiatry, Tokyo 187-8502, Japan; [12]Department of Paediatrics, University of Adelaide, Adelaide, South Australia 5000, Australia; [13]SA Clinical Genetics Service, SA Pathology at the Women's and Children's Hospital, North Adelaide, South Australia 5006, Australia; [14]Lotterywest State Biomedical Facility Genomics and School of Pathology and Laboratory Medicine, University of Western Australia, Perth, Western Australia 6000, Australia; [15]Department of Anatomical Pathology, Royal Perth Hospital, Perth, Western Australia 6000, Australia; [16]The Folkhälsan Institute of Genetics, Samfundet Folkhälsan, Biomedicum Helsinki, PB 63 (Haartmaninkatu 8), and Department of Medical Genetics, Haartman Institute, University of Helsinki, Helsinki 00014, Finland; [17]Department of Human Genetics, Yokohama City University, Graduate School of Medicine, 3-9 Fukuura, Kanazawa-ku, Yokohama 236-0004, Japan
*Correspondence: beggs@enders.tch.harvard.edu
http://dx.doi.org/10.1016/j.ajhg.2013.10.020. 

Therefore, we performed whole-exome sequencing (WES) combined, when applicable, with autozygome analysis to identify mutations in novel genes that underlie the disease pathology in a cohort of individuals affected with NM with unknown genetic diagnosis. All subjects were enrolled following informed consent and research was conducted according to the protocols approved by the Institutional Review Boards of the respective institutions in which these individuals were recruited. Molecular screening was performed on genomic DNA isolated from blood samples following standard protocols.

We performed whole-exome or whole-genome sequencing on a cohort of 60 unrelated NM probands through Boston Children's Hospital Gene Partnership facility. Molecular screening was performed on genomic DNA isolated from blood samples with standard protocols. Whole-blood DNA was subjected to solution capture (SureSelect Human All Exon V4, Agilent Technologies) to generate barcoded whole-exome sequencing libraries. Libraries were sequenced on an Illumina HiSeq 2000, employing paired end reads (100 bp × 2) to a mean target coverage of 96.5% and a mean read depth of 71.6. Alignment, variant calling, and annotation were performed with a custom informatics pipeline employing BWA,[14] Picard, and ANNOVAR[15] focusing on rare (<3% in db SNP135, 1000 Genomes Project Database, and the [EVS] National Heart, Lung, and Blood Institute Exome Sequencing Project Exome Variant Server) protein affecting changes in known and novel human disease genes. Alternatively, probands for families 203 and 832 were sequenced to greater than 50× depth by Axeq Technologies on an Illumina HiSeq 2000 following Agilent SureSelect Exome enrichment with their standard Exome Sequencing service. Whole-exome sequencing identified homozygous mutations of *KLHL41* in two unrelated families, suggesting this gene to be a candidate for NM. All *KLHL41* mutations are numbered relative to the mRNA sequence NM_006063.2 (where position 1 is the first base of the initiating MET codon) and protein NP_006054.2. Family 1 is a nonconsanguineous family of Vietnamese origin. Proband 203-1 is a 16-year-old female with an intermediate form of NM with a high-arched palate, dysarthria, and scoliosis who has required ventilatory support since childhood. WES identified an apparently homozygous c.103T>C transition in exon 1 resulting in a p.Cys35Arg substitution in this individual (Figure 1A). This variant was present as heterozygous in the father and absent in the mother. Copy number analysis in the affected region showed a heterozygous deletion in the mother and the proband, c.(?_-77)_(*602_?)del. Therefore, individual 203-1 is compound heterozygous for a deletion involving a portion of *KLHL41* and a KLHL41 p.Cys35Arg missense change. The second proband (832-1), who is adopted of Russian origin, is ambulant at age 12 and exhibits the typical congenital form of NM. WES identified a homozygous deletion of one base and an insertion of four bases c.459delinsACTC in the proband resulting in a single amino acid insertion, p.Ser153_Ala154insLeu in the protein (Figure 1A).

Whole-exome sequencing in probands with severe NM in Australian and Saudi Arabian cohorts resulted in identification of *KLHL41* mutations in two further families. The first (6462) is a consanguineous family of Persian origin from Afghanistan with one child (D12-203) affected with severe NM and four unaffected children (see Figure S1 available online). Homozygosity mapping was performed on the proband with the Illumina HumanCytoSNP-12 array, and the only known NM loci found within homozygous regions were *CFL2* (MIM 601443) and *NEB* (MIM 161650); however, both were excluded following Sanger sequencing, as was *ACTA1* (MIM 102610), which is the most common cause of simplex NM cases. WES of DNA from proband D12-203 was performed at the Lotterywest Sate Biomedical Facility Genomics Node, Royal Perth Hospital, Western Australia.[13] WES identified 453 heterozygous or homozygous variants. Application of the homozygosity data to the list of candidates reduced this to seven candidate variants. Two of these seven candidate variants were in skeletal-muscle-specific genes and of these the most likely candidate was a homozygous deletion within *KLHL41* (chr2: 170382132–170382139; c.1748_1755delAAGGAAAT, p.Lys583Thrfs*7) (Figure 1A). The deletion was confirmed by Sanger sequencing. Both parents and two unaffected siblings were heterozygous for the deletion, and two further unaffected siblings were homozygous for the normal allele.

Family 12DG1177, from a Saudi Arabian cohort is consanguineous (Figure S1). The male proband (12DG1177-1) was a newborn with severe hypotonia, dislocation of hips and knees, and facial dysmorphism in the form of micrognathia and cleft palate. There was a positive family history of two previous sibs who died of unknown causes soon after birth, as well as three healthy living sibs. The proband died of cardiorespiratory arrest shortly after intubation at less than 24 hr of age. Exome capture was performed with TruSeq Exome Enrichment kit (Illumina) as described earlier.[16] Only novel coding and splicing homozygous variants within the autozygome of the affected individual were considered. After filtering, 8,653 homozygous, coding, or splice variants were present, and autozygosity mapping, dbSNP, and analysis of 240 control Saudi exomes finally led to the identification of 18 candidate variants. The only truncating change was a single base deletion in *KLHL41* (c.641delA). This deletion was present in the coding region of exon 1 of *KLHL41* resulting in the frameshift change p.Asn214Thrfs*14 (Figure 1A).

Subsequent screening for *KLHL41* mutations in 116 individuals affected with severe, intermediate, or typical congenital forms of NM in the Boston and Australian NM Cohorts by Sanger sequencing identified a further family (D10-236) with compound heterozygous mutation (c.581_583delAAG, p.Glu194del and c.1238C>T, p.Ser413Leu) in proband. This individual is of Chinese

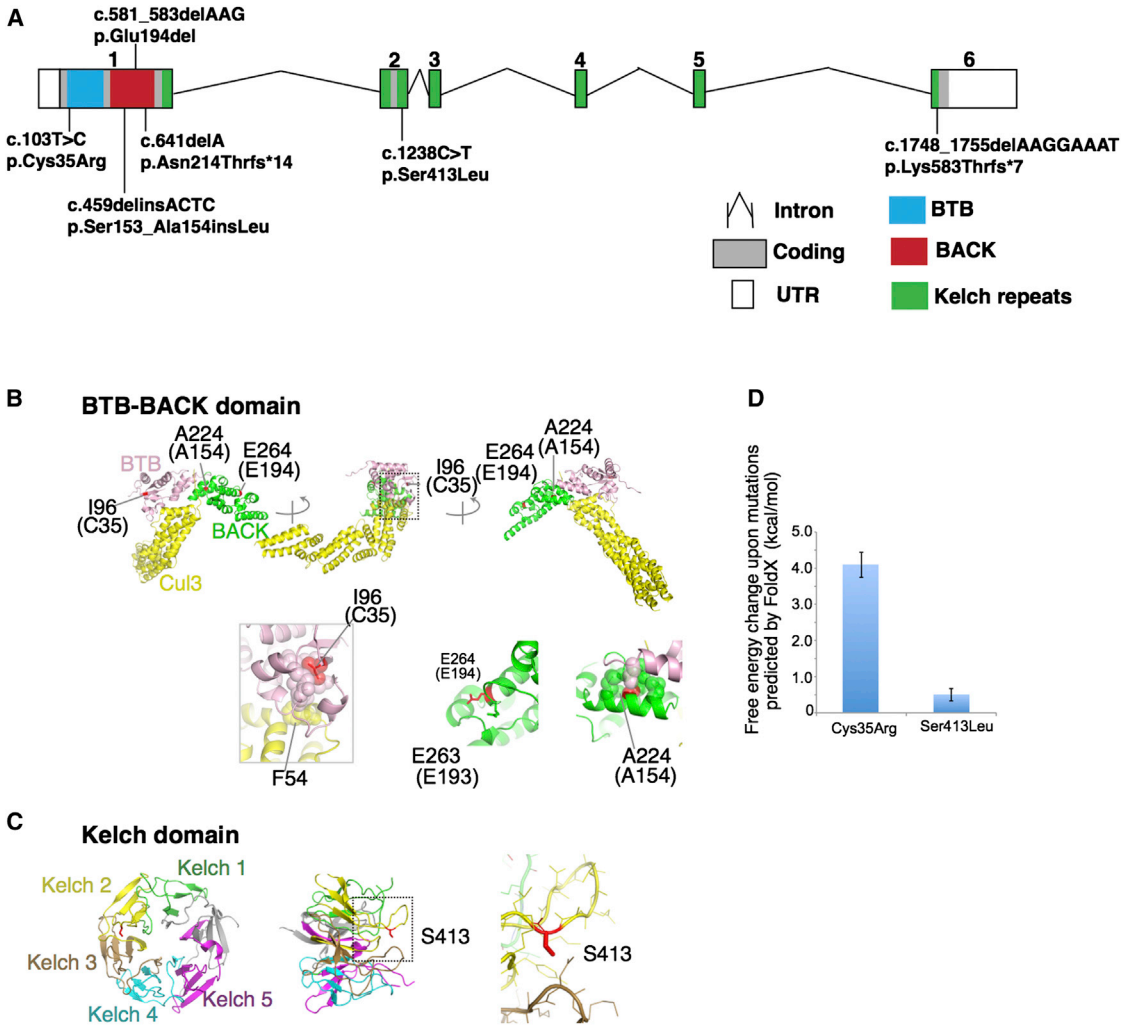


**Figure 1. Overview of Mutations in *KLHL41* and Their Effect on Protein Structure**

(A) Schematic representation of mutations in *KLHL41*. Boxes represent exons 1–6. Conserved domains of KLHL41 are indicated as follows: BTB (blue), BACK (red), and Kelch repeats (green). The BTB and BACK domains are encoded by exon 1 and the five Kelch repeats are encoded by exons 1–6.

(B and C) Crystal structures of the BTB-BACK domain of human Kelch-like protein (KLHL11) in complex with CUL3 (Protein Data Bank code 4AP2) (B) and the Kelch domain of rat KLHL41 (PDB code 2WOZ) (C). α helices, β strands, and loops are drawn as ribbons, arrows, and threads, respectively. The squared areas correspond to the close-up views in the insets. In (B), the BTB and BACK domains are colored pink and green, respectively, whereas CUL3 is colored yellow, except that Ile96, Ala224, and Glu264 (Cys35, Ala154, and Glu194 in human KLHL41, respectively) are colored red. The side chains of these residues and Glu263 (Glu193 in human KLHL41) are shown as sticks with the indications of amino acid numbers for human KLHL11 and those for human KLHL41 in parentheses. Side chains involved in hydrophobic cores around Ile96 and Ala224 are drawn in van der Waal's representation. In (C), the Kelch domain is color-coded to indicate each Kelch repeat, except that Ser413 is colored red. The side chain of Ser413 is shown as sticks. Molecular structures are drawn with PyMOL.

(D) Predicted free energy changes upon the substitutions of KLHL41 with FoldX software.

origin and exhibited the typical congenital form of NM. The detailed clinical features of affected individuals with mutations identified in *KLHL41* are presented in Table 1.

Overall, WES and Sanger sequencing resulted in identification of seven different mutations in Kelch-like family member 41 (*KLHL41*), previously known as *KBTBD10*, sarcosin, or *KRP1*, in affected NM individuals from five unrelated families (Figure 1A). Muscle histology was typical for NM: biopsies from probands of three different families (D12-203, 832-1, and 10-236) exhibited abnormal Gomori trichrome staining with presence of sarcoplasmic rods that varied from numerous small rods to fewer large rods in multiple myofibers (Figure 2A). No intranuclear rods or cores were seen. The missense changes identified in *KLHL41* are predicted to be pathogenic by polyphen, SIFT and pMUT and the mutated amino-acid residues are conserved in all representative species during evolution (Figure S2). The neighboring areas surrounding the sites of insertion or deletion are also relatively conserved, suggesting a structural or functional requirement for the altered amino acid residues (Figure S2). Sequencing of family members revealed that *KLHL41*

**Table1. Clinical Manifestations in Affected Individuals Harboring *KLHL41* Mutations**

| Proband ID | cDNA Change | Amino Acid Change | Clinical Category | Sex | Nationality | Pregnancy and Delivery | Alive at Age/Mobility/ Age at Death | Associated Features |
|---|---|---|---|---|---|---|---|---|
| **203-1** | c.103T>C c.(?_-77)_(*602_?)del | p.Cys35Arg Heterozygous p.0? Heterozygous | Intermediate | F | Vietnamese | Normal | 16 yrs, uses wheelchair (ambulant 24–36 mo) | Ventilated 24 hr from 5 yrs. High-arched palate, dysarthria Scoliosis |
| **832-1** | c.459delinsACTC | p.Ser153_Ala154insLeu Homozygous | Other forms (grade of severity: mild) | M | Russian | No data | 12 yrs, ambulant | Distal weakness > proximal distal contractures |
| **D10-236** | c.581_583delAAG<br>c.1238C>T | p.Glu194del Heterozygous<br>p.Ser413Leu Heterozygous | Typical form | M | Chinese | Normal - h 40 | 5 yrs, ambulant | VSD, finger contractures, focal renal echogenicity |
| **D12-203** | c.1748_1755del AAGGAAAT, | p.Lys583Thrfs*7 Homozygous | Fetal akinesia sequence | M | Persian | Polyhydramnios, breech presentation, emergency Cesarean section - h 31+2 | Died at 3 mo (active support discontinued) | Arthrogryposis, macrocephaly, hypospadias No antigravity movements at birth |
| **12DG1177** | c.641delA | p.Asn214Thrfs*14 Homozygous | Severe form Fetal akinesia sequence | M | Saudi Arabian | Fetal movements weak, breech presentation | Died during 1st day of life | Dislocation of hips and knees, cleft palate, micrognathia, narrow chest |

mutations showed a segregation pattern compatible with a recessive mode of inheritance in all families (Figure S1). Severe phenotypes associated with genetic null mutations and intermediate or typical congenital forms with mutations that should results in presence of residual protein, suggests a phenotype-genotype correlation in individuals affected with *KLHL41* mutations.

KLHL41 belongs to the family of BTB-Kelch domain-containing proteins.[17–20] Mutations in two other members of this family, *KBTBD13* (MIM 613727), and most recently *KLHL40* (MIM 615430), have been associated with a clinically distinct form of congenital myopathy exhibiting nemaline bodies, as well as multiminicores and severe NM, respectively.[12,13] To evaluate the impacts of the *KLHL41* mutations on the protein structure, we mapped them onto the crystal structures of the BTB-BACK domain of human KLHL11 in complex with human CUL3, a subunit of E3 ubiquitin ligases, (PDB code 4AP2)[21] and the Kelch domain of rat KLHL41 (PDB code 2WOZ),[22] analogous to those domains of human KLHL41. The Cys35 side chain is involved in a hydrophobic core of the BTB domain, which makes van der Waals contacts with Phe54 of Cul3 (Figure 1B). The p.Cys35Arg substitution present in affected individual 203-1 would likely destabilize the hydrophobic core and thereby impair the interaction with Cul3. This was supported by the FoldX result, in which free energy change upon the p.Cys35Arg substitution was predicted to be over 4 kcal/mol, which can be interpreted as considerable destabilization of a protein structure (Figure 1D; Figure S3).[23] In proband 832-1, a Leu residue is inserted between the amino acid positions 153 and 154 in the center of a helix, in which several residues are involved in a hydrophobic core of the BACK domain (Figure 1B). This amino acid insertion is likely to destabilize the BACK domain fold. In proband D10-236, the p.Ser413Leu substitution was mapped to a loop region, which is located near the substrate-binding region of the Kelch repeat 2 (Figure 1C; Figure S1B). A FoldX calculation predicted that the p.Ser413Leu substitution would have minimal effect on stability of the Kelch domain (Figure 1D). The effect of Glu194 deletion at the N-terminal end of an α helix can be compensated by the presence of Glu193 located in the loop (Figure 1B). Nonetheless, it cannot be excluded that the p.Ser413Leu and p.Glu194del changes alter the protein solubility or aggregate tendency and/or impair substrate binding. The conserved nature of the mutated KLHL41 domains, as well as the potential role of the mutations in disrupting those structural domains, supports the likely pathogenicity of these mutations.

The localization of KLHL41 in skeletal muscles was investigated by immunofluorescence of mouse FDB cultured myofibers and human skeletal muscle cryosections. Immunofluorescence with two different antibodies against N-terminal (Sigma, AV38732) and C-terminal parts of human KLHL41 (Abcam, ab66605) was performed, and z stacks were acquired by confocal microscopy as described

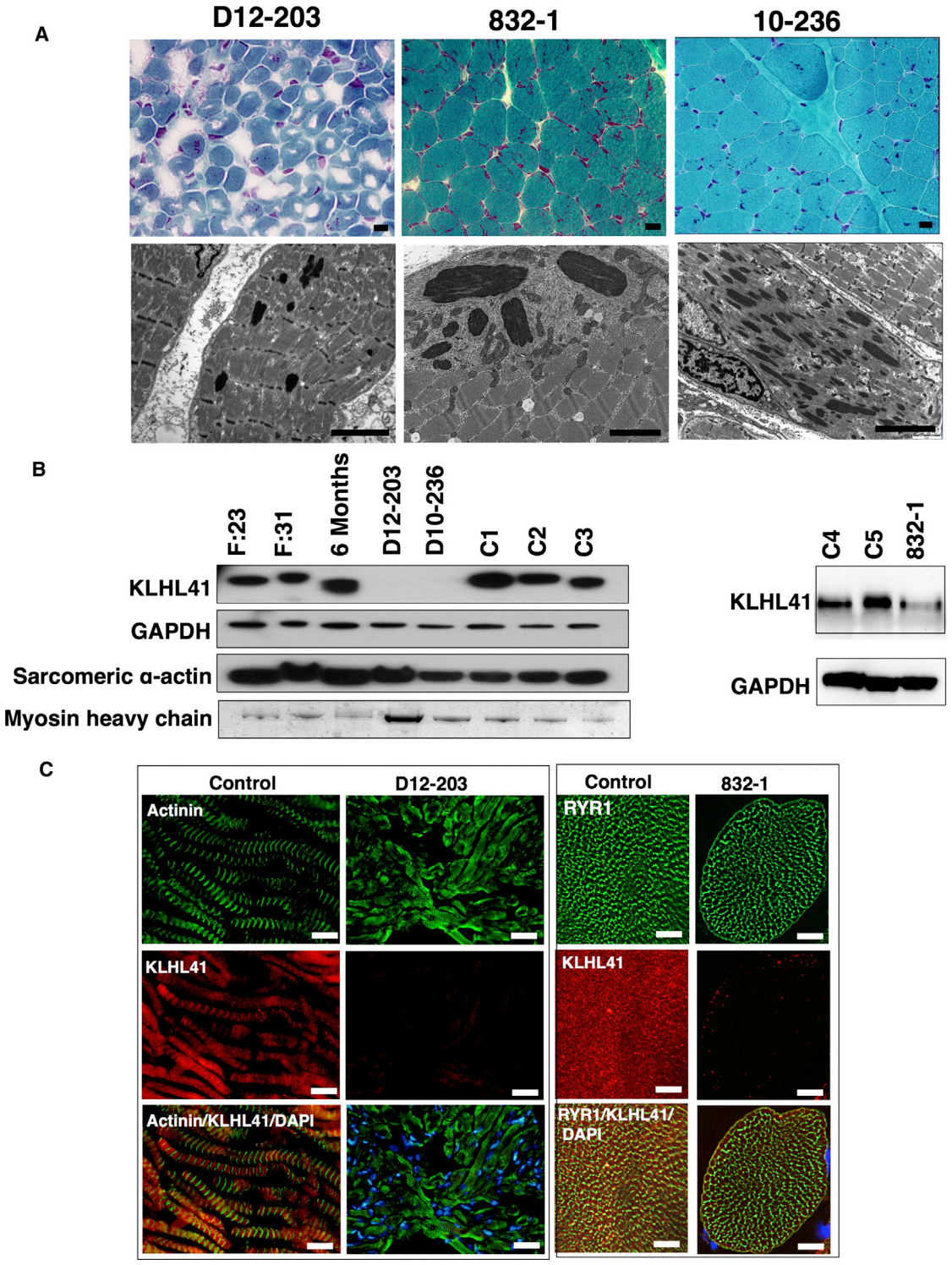


**Figure 2. Muscle Pathology and Expression of KLHL41 Levels and Localization in Muscle of Affected Individuals**

(A) Light microscopy of Gomori trichrome stained skeletal muscle from affected individuals with *KLHL41* mutations show cytoplasmic nemaline bodies (top panel). Electron microscopy of affected muscles reveals rods of variable frequency and size and severe myofibrillar disarray (bottom panels). (Scale bars represent 2 μm). Affected individuals' IDs are indicated at top.

(B) Immunoblotting analysis of KLHL41 levels in affected and unaffected muscles. A decrease in protein levels was observed in individuals with *KLHL41* mutations in comparison to normal control muscles. Immunoblotting with sarcomeric actin or Coomassie staining of myosin heavy chain showed no abnormal accumulation of sarcomeric proteins in affected muscles. Immunostaining for GAPDH was used for loading controls. Lanes: F:23, 23 week control fetus; F:30, 31 week control fetus; 6-month-old control baby, C1–C5 are normal age-matched control muscles.

(C) Immunofluorescence for KLHL41 in control and affected individual muscle biopsies showed highly reduced levels of KLHL41 in longitudinally oriented (left) or transverse sections (right) of skeletal muscles from affected individuals. Scale bars represent 50 μm.

previously.[24] Immunofluorescence with both antibodies resulted in similar staining patterns; however, due to lower background staining, the C-terminal antibody was used for further studies. Costaining with sarcomeric markers in longitudinal planes showed that KLHL41 staining predominated over the I-bands of the sarcomere and at perinuclear regions in human biopsies (Figure 2C) and murine cultured myofibers (Figure S4). Analysis of transverse sections of myofibers from control human biopsies revealed KLHL41 staining in a ring pattern around the myofibrils, generally colocalizing with ryanodine receptors (RYR1), which are a marker of the sarcoplasmic reticulum (Figure S5). Together, these observations suggest that KLHL41 localizes over (but not within) I bands, likely in association with the terminal cisternae of the sarcomplasmic reticulum (SR) and longitudinal vesicles of the SR present in the I-band area at the triadic regions (Figure S4). Colocalization studies with the ER marker protein disulfide isomerase (PDI) in myofibers and skeletal muscles further confirmed the localization of KLHL41 in SR-ER membranes (Figures S4). This overall localization pattern is most consistent with localization to the endoplasmic reticulum (ER) around myonuclei and to microdomains of the SR with ER characteristics.[25] Previous studies suggested that the closely related NM protein, KLHL40, localized at A-bands,[13] but double label immunofluorescence studies of both longitudinal and transverse sections here reveal that it appears colocalized with RYR1, around but not within the myofibrils in cultured myofibers and human skeletal muscles in a pattern overlapping, but not identical to, that of KLHL41 (Figures S4 and S5). These associations of proteins whose defects cause NM with the ER/SR contrasts with previously known NM proteins, all of which are sarcomeric thin filament components, with the exception of KBTBD13 whose localization is not well known.

In mouse tissues, immunoblotting detected KLHL41 in skeletal muscle and diaphragm (Figure S6). In cultured murine C2C12 cells, KLHL41 levels increased during differentiation to myotubes (Figure S6). Immunoblotting of affected skeletal muscle extracts revealed greatly reduced levels of KLHL41 in individuals with *KLHL41* mutations (Figure 2B) and immunofluorescence microscopy of affected individuals' skeletal muscles also showed that KLHL41 levels were greatly reduced in their myofibers (Figure 2C).

Cell culture studies have shown that KLHL41 interacts with nebulin, N-RAP (Nebulin-related anchoring protein), and actin in skeletal muscle and promotes the assembly of myofibrils.[26] KLHL41 regulates skeletal muscle differentiation as overexpression or knockdown inhibited C2C12 myoblast differentiation.[27] Knockdown of *Klhl41* in cultured cardiomyocytes resulted in sarcomeric disorganization with thickening of Z-lines as seen in NM.[28] However, the exact functions of KLHL41 in disease pathology are unknown. Recent studies have identified mutations in two other closely related family members *KBTBD13* and *KLHL40* as causes of NM suggesting the crucial requirement for several Kelch family proteins in skeletal muscle function.[12,13] To investigate the functional role of KLHL41 in vertebrate skeletal muscle development, we employed zebrafish as a model system. Zebrafish have two duplicated orthologs (*klhl41a* and *klhl41b*) that share ~80% similarity with *KLHL41*. Zebrafish whole-mount in situ hybridization was performed to study the spatio-temporal expression of these genes during zebrafish development as described previously.[29] Specifically, RNA probes specific for each Klhl41 gene were generated by amplification of the 3′ UTRs from a cDNA library of 2 day postfertilization (dpf) zebrafish embryos, followed by in vitro transcription to generate digoxigenin-labeled antisense transcripts (primer sequences are provided in Table S1). Whole-mount in situ hybridization showed ubiquitous expression of *klhl41a* during early development at 1 dpf, but by 2 dpf, *klhl41a* transcripts were virtually undetectable in the major axial skeletal muscles. In contract, *klhl41b* expression was predominantly seen in striated muscles, and strong expression in heart and skeletal muscles was observed throughout zebrafish development to at least 5 dpf (Figure 3A).

The effect of KLHL41 deficiency in zebrafish was studied by knocking down the Klhl41 genes with antisense morpholinos. Two independent morpholinos targeting an exon-intron spice site and translational start site were designed for both genes (morpholino sequences are provided in Table S2). As initial experiments with both morpholinos for each transcript resulted in similar phenotypes, we performed the remainder of our studies with the splice-site morpholinos (7 ng). *klhl41a* morphants exhibited leaner bodies, smaller eyes, and pericardial edema as seen in other myopathy models (n = 65–110) (Figure 3B).[30,31] Examination of 3 dpf morphants with polarized light showed reduced birefringence in axial skeletal muscles suggesting disorganized skeletal muscle structure (Figure 3B; Figure S7). Knockdown of *klhl41b* resulted in reduced birefringence without any other significant abnormalities (n = 82–132). Targeting both *klhl41a* and *klhl41b* (7 ng each) resulted in curved bodies with a 30% reduction in size along with small eyes and pericardial edema (n = 89–103), compared to fish injected with control morpholino (14ng). *klhl41a* morphant fish die by 3 dpf while *klhl41b* morphants typically did not survive past 5 dpf. Knockdown of both genes was lethal by 3 dpf. Double knockdown fish exhibited severely disorganized muscle (measured by reduced birefringence) compared to controls and either of the single knockdowns. RT-PCR and immunoblotting confirmed the knockdown of *klhl41a* and *klhl41b* transcripts and a reduction in protein levels (Figures 3C and 3D). Overexpression of human *KLHL41* mRNA in the double morphants resulted in a significant increase in the number of surviving fish with normal birefringence suggesting the specificity of morpholino injections and demonstrating the ability of this single evolutionary ortholog to complement both zebrafish genes (Figure 3E). Behavioral characterization of 3

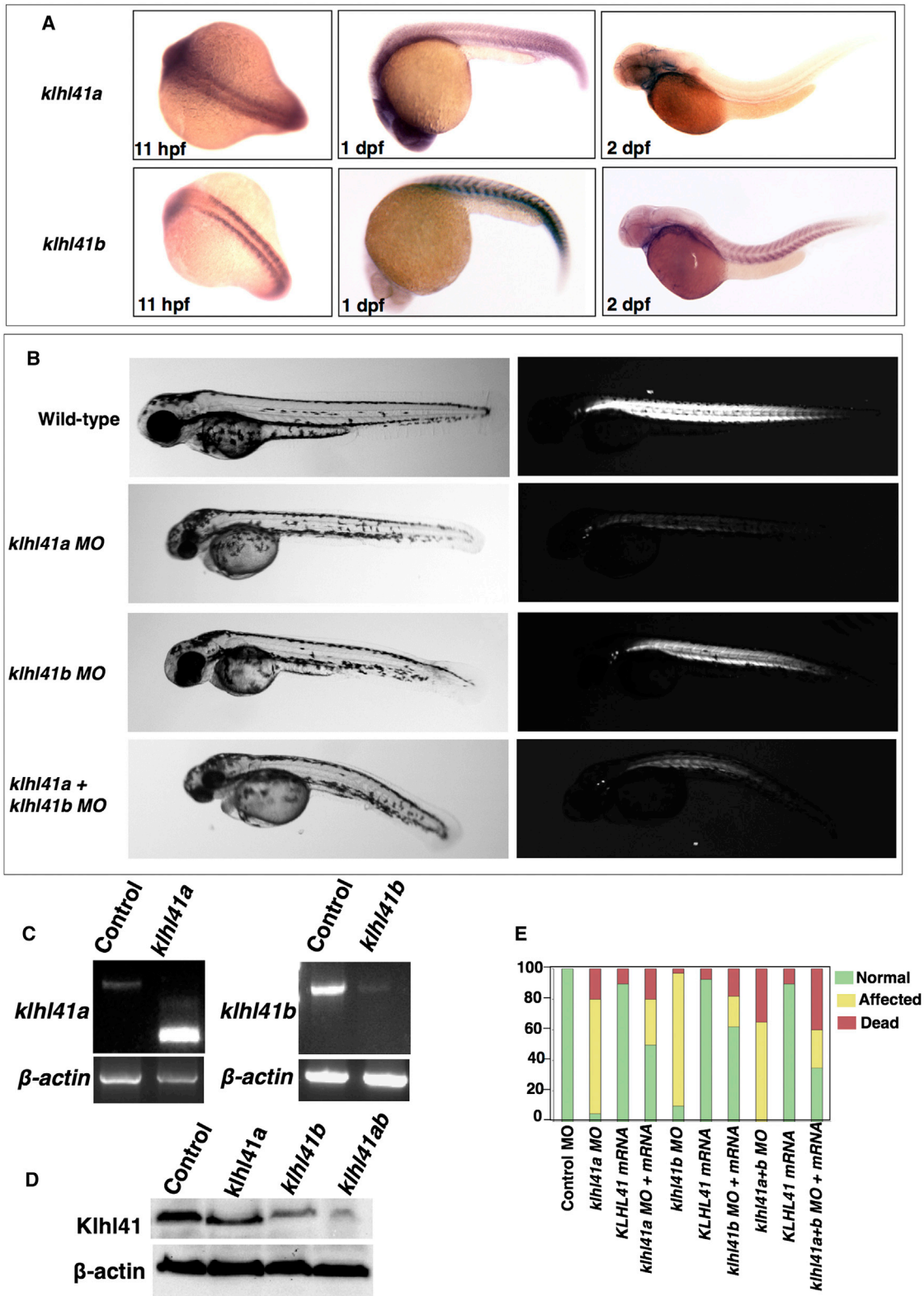


**Figure 3. Characterization and Knockdown of Zebrafish Orthologs of *KLHL41***

(A) In situ hybridization of the zebrafish Klhl41 genes shows early expression during myogenesis in developing somites (11 hr after fertilization). *Klhl41a* is expressed in brain, eyes, and muscle at 1 dpf. Later in development expression is largely restricted to brain and heart (2 dpf), although low levels of expression in axial slow skeletal myofibers cannot be excluded due to limited sensitivity of the assay. *Klhl41b* expression is localized to skeletal muscle and heart at all developmental stages (1–2 dpf).

(B) Knockdown of Klhl41 genes in zebrafish using antisense morpholinos results in myopathic changes. Live microscopy of zebrafish embryos at 3 dpf reveals leaner and smaller bodies in comparison to wild-type (WT) fish. Under polarized microscopy, zebrafish embryos

*(legend continued on next page)*

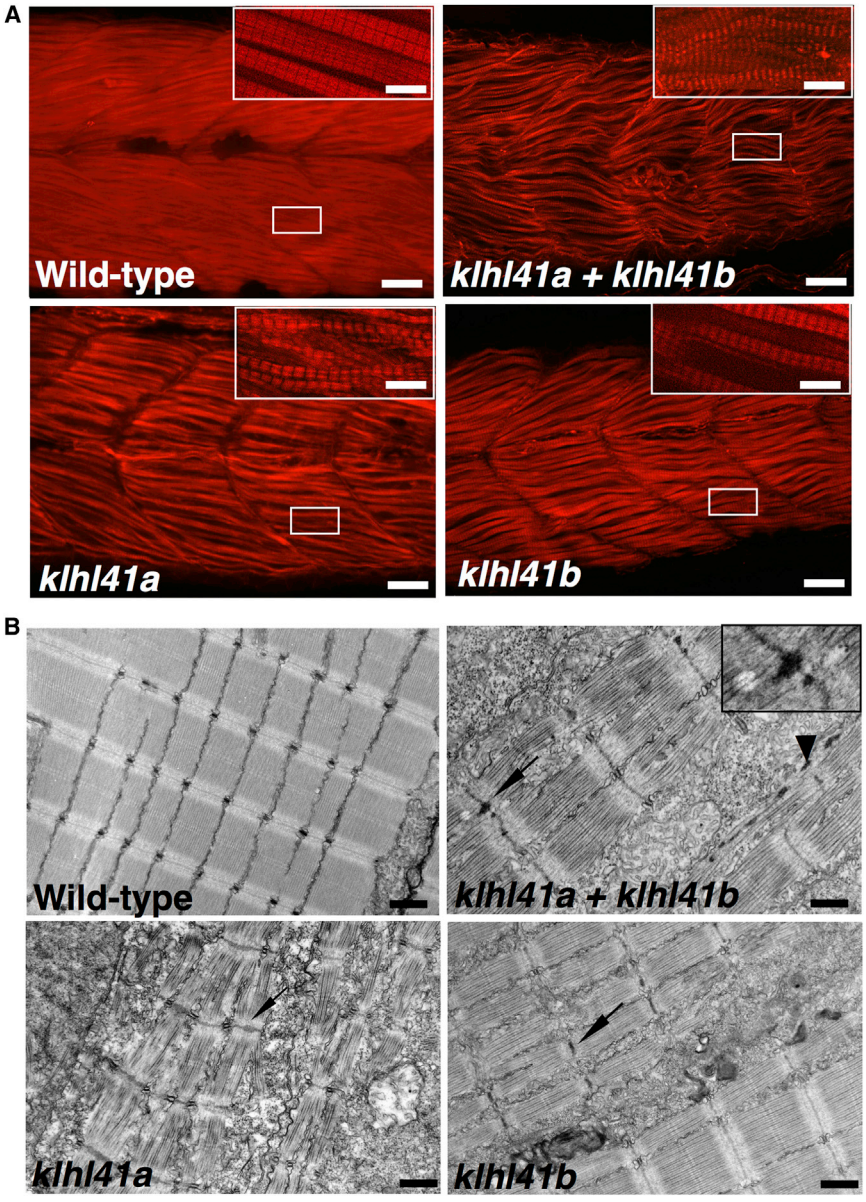


**Figure 4. Loss of *klhl41* Function in Zebrafish Recapitulates the Disease Pathology of Human Nemaline Myopathies**
(A) Whole-mount staining of 3 dpf zebrafish embryos with phalloidin showed extensive myofibrillar disarray of myofibers in *klhl41* morphant fish (scale bar represents 2 μm). Three dpf embryos fixed in 4% paraformaldehyde were incubated with phalloidin (Invitrogen, A12380, 1:40) overnight at 4°C. Skeletal muscles of klhl41-deficient embryos were smaller and exhibited an overall reduction of myofibrillar organization (inset, high magnification).
(B) Electron microscopy of klhl41-deficient skeletal muscle revealed thickened Z-lines in *klhl41a* or *klhl41b* morphants. In addition, skeletal muscle of double knockdown fish contained electron dense bodies, reminiscent of nascent nemaline rods (arrowhead, nemaline bodies like structures; arrow, thickened Z-lines) (scale bar represents 1 μm).

dpf morphant fish, knocked down for either or both Klhl41 genes, using the touch-evoked response assay showed significantly diminished motility in comparison to control fish (WT fish: 5.74 ± 0.98 cm/0.1 s; *klhl41a*: 1.32 ± 0.61 cm/0.1 s; *klhl41b*: 2.00 ± 0.49 cm/0.1 s; *klhl41ab*: 0.73 ± 0.39 cm/0.1 s), suggesting a significant degree of overall muscle weakness (Movies S1, S2, S3, and S4).[32] To visualize abnormalities in sarcomeric architecture, whole-mount staining of morphant fish and control zebrafish embryos was performed with phalloidin to stain the actin-thin filaments. Although well-organized myofibrillar striations (i.e., sarcomeres) were observed, the myofibrils in *klhl41* morphants tended to be thinner and were highly disorganized relative to control fish (Figure 4A). The myofibrilar disorganization in *klhl41* morphants was also evident by evaluation of ultrathin toluidine blue sections of control and morphant fish (Figure S7). The main diagnostic feature of NM is the presence of nemaline rods with or without Z-line streaming in skeletal muscle. Ultrastructural examination of zebrafish skeletal muscle by electron microscopy showed Z-line thickening in both *klhl41a* and *klhl41b* morphant fish (Figure 4B). Knockdown of both *klhla* and *klhl41b* resulted in the presence of numerous electron-dense structures, reminiscent of small or nascent nemaline bodies, in addition to Z-line thickening (Figure 4B). Given the differences in temporal expression of *klhl41a* (early embryogenesis) and *klhl41b*

exhibit a reduction in birefringence in morphant fish, quantified in ImageJ as described (WT controls: 100% ± 5.9% *klhl41a*: 23% ± 3.0%; *klhl41b*: 31% ± 8.2%; *klhl41ab*: 16% ± 4.2%). Double knockdown fish show a more severe skeletal muscle phenotype than single morphants.
(C) RT-PCR analysis showed knockdown of normal transcripts in the morphant fish.
(D) Immunoblot analysis showed reduction in Klhl41 levels in *klhl41a*, *klhl41b*, and *klhl41ab* fish. Klhl41 antibody recognizes both klhl41a and klhl41b and therefore show immunoreactibility to the other gene in the single morphants that is highly reduced in double morphants.
(E) Overexpression of human *KLHL41* mRNA restores the skeletal muscle phenotypes of *klhl41a/b* single and double morphants suggesting morpholino specificity. The mRNA concentration used to rescue were as follows: *klhl41a* (50 pg), *klhl41b* (75 pg), *klhl41a+b* (60 pg of each).

(maintained later in development), and the high degree of structural and functional conservation (both are rescued by the single human transcript), it is likely that increased severity of *klhl41a* morphants is due to this being the predominant embryonic isoform at the early stages targeted by morpholino injections.

Extensive skeletal muscle disorganization associated with sarcomeric abnormalities in morphant fish points toward a function of KLHL41 in skeletal muscle development and maintenance. Mutations affecting the closely related BTB-Kelch family member KLHL40 have recently also been reported to cause nemaline myopathy.[13] While *KLHL40* mutations resulted in a severe clinical presentation in most of the affected individuals, KLHL41 abnormalities are associated with a spectrum of phenotypes from severe with neonatal death, to survival into late childhood. However, no significant differences were seen in skeletal muscle pathology. KLHL40 contains a putative nuclear localization sequence (NLS) and is expressed throughout muscle differentiation, whereas KLHL41 lacks NLS and is expressed in late differentiation (Figure S8).[13] KLHL41 and many other BTB domain-containing Kelch family members are known to interact with Cul3 ubiquitin ligase to form functional ubiquitination complexes with proteins targeted for degradation.[21,33] KLHL41, which has been shown to interact with nebulin,[34] is now the third BTB-Kelch family member to be identified as a cause of NM when mutated. We hypothesize that improper surveillance and degradation of aberrant thin-filament proteins might explain the convergent pathological and clinical phenotypes associated with mutations of thin filament and BTB-Kelch family member genes in NM.

## Supplemental Data

Supplemental Data include eight figures, two tables, and four movies and can be found with this article online at http://www.cell.com/AJHG/home.

## Acknowledgments

We are grateful to the many NM affected individuals and their families, and to their treating physicians, for their participation in this research. Whole-exome sequencing was made possible through the generous support and assistance of David Margulies and the entire staff of The Gene Partnership Project at Boston Children's Hospital. We would like to thank Pankaj Agrawal and Wen-Hann Tan for many helpful discussions during the course of this work. We are thankful to Louise Trakimas of the electron microscope facility at Harvard Medical School for excellent help with zebrafish histology, and the Genotyping and Sequencing Core Facilities at KFSHRC for their technical help. V.A.G. is supported by K01 AR062601 from the National Institute of Arthritis and Musculoskeletal and Skin Diseases of National Institute of Health. This work was also supported by the Muscular Dystrophy Association of USA (MDA201302), National Institutes of Health grant from the National Institute of Arthritis and Musculoskeletal and Skin Diseases R01 AR044345, the AUism Charitable Foundation, and A Foundation Building Strength (to A.H.B.); National Health and Medical Research Council of Australia Early Career Researcher Fellowship #1035955 (to G.R.); Research Fellowship APP1002147 and Project Grant APP1022707(to N.G.L.); the Association Française contre les Myopathies (#15734), Dubai-Harvard Foundation for Medical Research Collaborative Research Grant (to F.S.A.); a UWA Collaborative Research Award (G.R.); and the Great Ormond Street Hospital Children's Charity (to F.M.). E.J.T. and K.S.Y. are supported by University of Western Australia Postgraduate Awards. DNA sequencing was performed by the Boston Children's Hospital Genomics Program Molecular Genetics Core, and confocal microscopy was performed at Boston Children's Hospital Intellectual and Developmental Disability Research Center Imaging Core, both supported by National Institutes of Health grant P30 HD18655. The funders had no role in study design, data collection and analysis, decision to publish, or preparation of the manuscript.

Received: August 9, 2013
Revised: October 15, 2013
Accepted: October 22, 2013
Published: November 21, 2013

## Web Resources

The URLs for data presented herein are as follows:

1000 Genomes, http://browser.1000genomes.org
dbSNP, http://www.ncbi.nlm.nih.gov/projects/SNP/
NHLBI Exome Sequencing Project (ESP) Exome Variant Server, http://evs.gs.washington.edu/EVS/
Online Mendelian Inheritance in Man (OMIM), http://www.omim.org/
Picard, http://picard.sourceforge.net/
Pymol, http://www.pymol.org

## References

1. Wallgren-Pettersson, C., Sewry, C.A., Nowak, K.J., and Laing, N.G. (2011). Nemaline myopathies. Semin. Pediatr. Neurol. *18*, 230–238.
2. Ryan, M.M., Schnell, C., Strickland, C.D., Shield, L.K., Morgan, G., Iannaccone, S.T., Laing, N.G., Beggs, A.H., and North, K.N. (2001). Nemaline myopathy: a clinical study of 143 cases. Ann. Neurol. *50*, 312–320.
3. Wallgren-Pettersson, C. (2002). Nemaline and myotubular myopathies. Semin. Pediatr. Neurol. *9*, 132–144.
4. Sewry, C.A. (2008). Pathological defects in congenital myopathies. J. Muscle Res. Cell Motil. *29*, 231–238.
5. Hutchinson, D.O., Charlton, A., Laing, N.G., Ilkovski, B., and North, K.N. (2006). Autosomal dominant nemaline myopathy with intranuclear rods due to mutation of the skeletal muscle ACTA1 gene: clinical and pathological variability within a kindred. Neuromuscul. Disord. *16*, 113–121.
6. Pelin, K., Hilpelä, P., Donner, K., Sewry, C., Akkari, P.A., Wilton, S.D., Wattanasirichaigoon, D., Bang, M.L., Centner, T., Hanefeld, F., et al. (1999). Mutations in the nebulin gene associated with autosomal recessive nemaline myopathy. Proc. Natl. Acad. Sci. USA *96*, 2305–2310.
7. Nowak, K.J., Wattanasirichaigoon, D., Goebel, H.H., Wilce, M., Pelin, K., Donner, K., Jacob, R.L., Hübner, C., Oexle, K., Anderson, J.R., et al. (1999). Mutations in the skeletal muscle

alpha-actin gene in patients with actin myopathy and nemaline myopathy. Nat. Genet. *23*, 208–212.
8. Laing, N.G., Wilton, S.D., Akkari, P.A., Dorosz, S., Boundy, K., Kneebone, C., Blumbergs, P., White, S., Watkins, H., Love, D.R., et al. (1995). A mutation in the alpha tropomyosin gene TPM3 associated with autosomal dominant nemaline myopathy. Nat. Genet. *9*, 75–79.
9. Tajsharghi, H., Ohlsson, M., Lindberg, C., and Oldfors, A. (2007). Congenital myopathy with nemaline rods and cap structures caused by a mutation in the beta-tropomyosin gene (TPM2). Arch. Neurol. *64*, 1334–1338.
10. Agrawal, P.B., Greenleaf, R.S., Tomczak, K.K., Lehtokari, V.L., Wallgren-Pettersson, C., Wallefeld, W., Laing, N.G., Darras, B.T., Maciver, S.K., Dormitzer, P.R., and Beggs, A.H. (2007). Nemaline myopathy with minicores caused by mutation of the CFL2 gene encoding the skeletal muscle actin-binding protein, cofilin-2. Am. J. Hum. Genet. *80*, 162–167.
11. Johnston, J.J., Kelley, R.I., Crawford, T.O., Morton, D.H., Agarwala, R., Koch, T., Schäffer, A.A., Francomano, C.A., and Biesecker, L.G. (2000). A novel nemaline myopathy in the Amish caused by a mutation in troponin T1. Am. J. Hum. Genet. *67*, 814–821.
12. Sambuughin, N., Yau, K.S., Olivé, M., Duff, R.M., Bayarsaikhan, M., Lu, S., Gonzalez-Mera, L., Sivadorai, P., Nowak, K.J., Ravenscroft, G., et al. (2010). Dominant mutations in KBTBD13, a member of the BTB/Kelch family, cause nemaline myopathy with cores. Am. J. Hum. Genet. *87*, 842–847.
13. Ravenscroft, G., Miyatake, S., Lehtokari, V.L., Todd, E.J., Vornanen, P., Yau, K.S., Hayashi, Y.K., Miyake, N., Tsurusaki, Y., Doi, H., et al. (2013). Mutations in KLHL40 are a frequent cause of severe autosomal-recessive nemaline myopathy. Am. J. Hum. Genet. *93*, 6–18.
14. Li, H., and Durbin, R. (2009). Fast and accurate short read alignment with Burrows-Wheeler transform. Bioinformatics *25*, 1754–1760.
15. Wang, K., Li, M., and Hakonarson, H. (2010). ANNOVAR: functional annotation of genetic variants from high-throughput sequencing data. Nucleic Acids Res. *38*, e164.
16. Alkuraya, F.S. (2012). Discovery of rare homozygous mutations from studies of consanguineous pedigrees. Curr Protoc Hum Genet. *Chapter 6*, Unit 6, 12.
17. Adams, J., Kelso, R., and Cooley, L. (2000). The kelch repeat superfamily of proteins: propellers of cell function. Trends Cell Biol. *10*, 17–24.
18. Dhanoa, B.S., Cogliati, T., Satish, A.G., Bruford, E.A., and Friedman, J.S. (2013). Update on the Kelch-like (KLHL) gene family. Hum. Genomics *7*, 13.
19. du Puy, L., Beqqali, A., van Tol, H.T., Monshouwer-Kloots, J., Passier, R., Haagsman, H.P., and Roelen, B.A. (2012). Sarcosin (Krp1) in skeletal muscle differentiation: gene expression profiling and knockdown experiments. Int. J. Dev. Biol. *56*, 301–309.
20. Gray, C.H., McGarry, L.C., Spence, H.J., Riboldi-Tunnicliffe, A., and Ozanne, B.W. (2009). Novel beta-propeller of the BTB-Kelch protein Krp1 provides a binding site for Lasp-1 that is necessary for pseudopodial extension. J. Biol. Chem. *284*, 30498–30507.
21. Canning, P., Cooper, C.D., Krojer, T., Murray, J.W., Pike, A.C., Chaikuad, A., Keates, T., Thangaratnarajah, C., Hojzan, V., Marsden, B.D., et al. (2013). Structural basis for Cul3 protein assembly with the BTB-Kelch family of E3 ubiquitin ligases. J. Biol. Chem. *288*, 7803–7814.
22. Spence, H.J., Johnston, I., Ewart, K., Buchanan, S.J., Fitzgerald, U., and Ozanne, B.W. (2000). Krp1, a novel kelch related protein that is involved in pseudopod elongation in transformed cells. Oncogene *19*, 1266–1276.
23. Guerois, R., Nielsen, J.E., and Serrano, L. (2002). Predicting changes in the stability of proteins and protein complexes: a study of more than 1000 mutations. J. Mol. Biol. *320*, 369–387.
24. Lawlor, M.W., Alexander, M.S., Viola, M.G., Meng, H., Joubert, R., Gupta, V., Motohashi, N., Manfready, R.A., Hsu, C.P., Huang, P., et al. (2012). Myotubularin-deficient myoblasts display increased apoptosis, delayed proliferation, and poor cell engraftment. Am. J. Pathol. *181*, 961–968.
25. Kaisto, T., and Metsikkö, K. (2003). Distribution of the endoplasmic reticulum and its relationship with the sarcoplasmic reticulum in skeletal myofibers. Exp. Cell Res. *289*, 47–57.
26. Lu, S., Carroll, S.L., Herrera, A.H., Ozanne, B., and Horowits, R. (2003). New N-RAP-binding partners alpha-actinin, filamin and Krp1 detected by yeast two-hybrid screening: implications for myofibril assembly. J. Cell Sci. *116*, 2169–2178.
27. Paxton, C.W., Cosgrove, R.A., Drozd, A.C., Wiggins, E.L., Woodhouse, S., Watson, R.A., Spence, H.J., Ozanne, B.W., and Pell, J.M. (2011). BTB-Kelch protein Krp1 regulates proliferation and differentiation of myoblasts. Am. J. Physiol. Cell Physiol. *300*, C1345–C1355.
28. Greenberg, C.C., Connelly, P.S., Daniels, M.P., and Horowits, R. (2008). Krp1 (Sarcosin) promotes lateral fusion of myofibril assembly intermediates in cultured mouse cardiomyocytes. Exp. Cell Res. *314*, 1177–1191.
29. Gupta, V., Discenza, M., Guyon, J.R., Kunkel, L.M., and Beggs, A.H. (2012). α-Actinin-2 deficiency results in sarcomeric defects in zebrafish that cannot be rescued by α-actinin-3 revealing functional differences between sarcomeric isoforms. FASEB J. *26*, 1892–1908.
30. Dowling, J.J., Vreede, A.P., Low, S.E., Gibbs, E.M., Kuwada, J.Y., Bonnemann, C.G., and Feldman, E.L. (2009). Loss of myotubularin function results in T-tubule disorganization in zebrafish and human myotubular myopathy. PLoS Genet. *5*, e1000372.
31. Gupta, V.A., Kawahara, G., Myers, J.A., Chen, A.T., Hall, T.E., Manzini, M.C., Currie, P.D., Zhou, Y., Zon, L.I., Kunkel, L.M., and Beggs, A.H. (2012). A splice site mutation in laminin-α2 results in a severe muscular dystrophy and growth abnormalities in zebrafish. PLoS ONE *7*, e43794.
32. Smith, L.S., Beggs, A.H., and Gupta, V.A. (2013). Analysis of skeletal muscle defects in larval zebrafish by birefringence and touch-evoke escape response assays. J. Vis. Exp. *82*, e50925. http://dx.doi.org/10.3791/50925.
33. Zhang, D.D., Lo, S.C., Sun, Z., Habib, G.M., Lieberman, M.W., and Hannink, M. (2005). Ubiquitination of Keap1, a BTB-Kelch substrate adaptor protein for Cul3, targets Keap1 for degradation by a proteasome-independent pathway. J. Biol. Chem. *280*, 30091–30099.
34. Spence, H.J., McGarry, L., Chew, C.S., Carragher, N.O., Scott-Carragher, L.A., Yuan, Z., Croft, D.R., Olson, M.F., Frame, M., and Ozanne, B.W. (2006). AP-1 differentially expressed proteins Krp1 and fibronectin cooperatively enhance Rho-ROCK-independent mesenchymal invasion by altering the function, localization, and activity of nondifferentially expressed proteins. Mol. Cell. Biol. *26*, 1480–1495.